

Essential O₂-responsive genes of *Pseudomonas aeruginosa* and their network revealed by integrating dynamic data from inverted conditions†

Cite this: DOI: 10.1039/c3ib40180d

Feng Q. He,^{*ab} Wei Wang,^{ac} Ping Zheng,^{‡a} Padhmanand Sudhakar,^c Jibin Sun^{‡a} and An-Ping Zeng^{*ac}

Identification of the gene network through which *Pseudomonas aeruginosa* PAO1 (PA) adapts to altered oxygen-availability environments is essential for a better understanding of stress responses and pathogenicity of PA. We performed high-time-resolution (HTR) transcriptome analyses of PA in a continuous cultivation system during the transition from high oxygen tension to low oxygen tension (HLOT) and the reversed transition from low to high oxygen tension (LHOT). From those genes responsive to both transient conditions, we identified 85 essential oxygen-availability responsive genes (EORGs), including the expected ones (arcDABC) encoding enzymes for arginine fermentation. We then constructed the regulatory network for the EORGs of PA by integrating information from binding motif searching, literature and HTR data. Notably, our results show that only the sub-networks controlled by the well-known oxygen-responsive transcription factors show a very high consistency between the inferred network and literature knowledge, e.g. 87.5% and 83.3% of the obtained sub-network controlled by the anaerobic regulator (ANR) and a quorum sensing regulator RhIR, respectively. These results not only reveal stringent EORGs of PA and their transcription regulatory network, but also highlight that achieving a high accuracy of the inferred regulatory network might be feasible only for the apparently affected regulators under the given conditions but not for all the expressed regulators on a genome scale.

Received 2nd September 2013,
Accepted 21st November 2013

DOI: 10.1039/c3ib40180d

www.rsc.org/ibiology

Insight, innovation, integration

We here identified essential responsive genes of *Pseudomonas aeruginosa* (PA) toward oxygen availability and constructed a reliable transcription regulatory network controlling them for a better understanding of stress responses and pathogenicity of PA. The success in constructing the reliable transcription regulatory network was achieved by integrating high-time-resolution dynamic transcriptome data measured from two inverted oxygen-availability transitions, transcription factor binding motif information and literature knowledge of perturbation effect experiments of transcription factors. This is the first work to construct a transcription network by integrating high-time-resolution data from two inverted conditions. As demonstrated here, it is very difficult to construct such a reliable transcription regulatory network without such an integrated analysis based on high-time-resolution dynamic transcriptome data measured from inverted conditions.

Introduction

Pseudomonas aeruginosa PAO1 (PA), a prominent opportunistic human pathogen, is a facultative anaerobe able to occupy a

wide range of environmental niches, where oxygen availability is a critical factor that determines the survival and growth modes of PA.¹ A number of studies have revealed that oxygen availability affects the expression of a wealth of genes associated with different metabolic pathways and cellular functions of PA, including quorum sensing, biofilm formation, antibiotic tolerance and even small RNAs that contribute to the persistence of this opportunistic pathogen.^{2–5} Many of the genes have been reported to be under the regulation of the anaerobic regulator (ANR). As the name indicates, ANR, the product of the *anr* gene, is a key regulator of many anaerobic responses.^{6,7} In addition to traditional individual-gene-focused investigations, some studies have investigated PA using whole-genome

^a Helmholtz Centre for Infection Research, D-38124, Braunschweig, Germany

^b Luxembourg Centre for Systems Biomedicine (LCSB), University of Luxembourg, L-4362, Esch-Belval, Luxembourg. E-mail: feng.he@uni.lu

^c Institute of Bioprocess and Biosystems Engineering, Hamburg University of Technology, D-21073 Hamburg, Germany. E-mail: Aze@tuhh.de

† Electronic supplementary information (ESI) available. See DOI: 10.1039/c3ib40180d

‡ Current address: Tianjin Institute of Industrial Biotechnology, Chinese Academy of Sciences, Tianjin 300308, China.

transcriptome analyses. For example, transcriptome analyses have been performed to study PA responses to different challenges such as iron limitation, oxidative stress, quorum sensing, biofilm formation, and others.⁸ Based on such transcriptome analyses, efforts have been initiated to gain a systematic understanding of the responses of PA to oxygen availability, such as the approach of defining ANR and DNR regulons.⁹ However, many of the gene expression analyses have primarily focused on long-term effects of perturbations.^{10–13} But responses of bacteria to environmental stimuli can be very fast and dynamic, which cannot be adequately captured by static measurements or even by long-time-interval dynamic measurements.^{14,15} In addition, many of the studies were based on shaking flask cultures where aerobic or anaerobic conditions were not clearly defined. Furthermore, most of the current studies aim to identify the genes responsive to either anaerobic (or microaerobic) or high oxygen conditions. We believe that the EORGs shall respond to environmental changes not only towards low oxygen levels but also towards high oxygen conditions, analogous to the classic cases where individual genes respond to both the loss-of- and gain-of-function perturbations in molecular biology.

We have previously studied physiological responses and gene regulations of PA toward the availability of iron and/or oxygen in a computer-controlled bioreactor system with exactly defined conditions.^{16–20} In this study we extend our work with *P. aeruginosa* to a network-based investigation of genome-scale dynamic gene expression regarding O₂ variation. For this purpose, we measured and analyzed a HTR transcriptome under two inverted transitions, from oxygen repletion to oxygen depletion conditions and the inverted perturbation. We aim to identify the EORGs by focusing on the overlap of responsive genes under the two inverted transition conditions. In order to better understand the molecular mechanisms through which PA adapts to altered oxygen-availability environments, we further set out to identify the transcription regulatory network controlling these EORGs. Many efforts have already been made to construct quality transcription regulatory networks by developing various approaches and/or applying to various organisms.^{21–26} However, it is still a challenging task to infer reliable and experimentally-testable regulatory networks mainly based on transcription data without combining other sufficient information.^{21,23,27} In fact, a recent extensive evaluation demonstrates that most of the unsupervised inference methods show low prediction accuracies and supervised and semi-supervised approaches achieve higher accuracies.²⁸

In this work, we have constructed a reliable transcription regulatory network of PA responsive to oxygen availability by combining prior literature information (genes affected by mutation or overexpression of given transcription factors (TFs)) and binding motif searching as well as by focusing on the EORGs. Taken together, the specific points of this work are: (i) measurement of the HTR transcriptome sampled with an interval of 5 or 10 minutes under two inverted conditions in a computer-controlled cultivation system, (ii) identification of the genes responsive to both conditions by treating the two HTR data sets as inverted repetitions, (iii) construction of a

reliable transcription regulatory network by combining binding motif searching and information on genes affected by perturbation experiments of given TFs.

Results and discussion

Identification of EORGs

With the well-accepted conjecture that essential genes responsive to loss-of-function of a TF shall also respond to gain-of-function of the TF and that the expression change of these responsive genes is inverted between two reversed perturbations, we aim to identify EORGs by searching for genes affected under both HLOT and LHOT conditions. To meet these criteria, we chose genes that not only showed certain expression variation, *e.g.*, change fold equal to or larger than 1.5 among any two time points in the time-course measurement of both HLOT and LHOT conditions, but also showed significantly inverted transcription change patterns over time between the two conditions (negatively correlated by the Pearson correlation coefficient, $P \leq 0.05$, Fig. 1A). It is clear that a significant inverted correlation cannot be easily obtained by chance between two inverted conditions from 14 continuous sampling points with such a short time interval. An inverted change pattern revealed by such a strategy is much closer to the truth than that shown by the studies in which only a couple of time points have been measured. To this end, we found 85 EORGs (Fig. 1B). To more efficiently analyze these EORGs, we employed the hierarchical clustering approach based on the concatenated data of the two inverted conditions. Several groups were identified, which showed different dynamics of the transitions (Fig. 1B). We here only demonstrated some of the EORGs (Fig. 1C). We did not simply discuss them by groups, which were closely clustered together, but chose genes from different groups, which nonetheless still showed a general similar pattern by ignoring very detailed dynamics, to represent more genes. As shown in Fig. 1C, some genes (*e.g.*, PA0167, PA1963 and PA3530) gradually decreased in their expression level with time under the HLOT conditions while gradually increasing under the LHOT conditions. Some genes (*e.g.*, PA0315, PA1986 and PA1250) first decreased their transcription expression then gradually increased back during the HLOT transition and showed an inverted change during the LHOT transition. This type of expression change clearly indicates a negative feedback involved in the mRNA expression regulation of these genes. From the experimental design point of view, it is almost impossible to catch such dynamic response patterns without a high-frequency measurement.¹⁴ Other genes (PA4655 and PA1249, Fig. 1C) first increased their transcription levels and then slowly decreased to base levels under the HLOT conditions whereas they showed an inverted change in the LHOT transition. Even for this type of pattern change, the dynamics also differs from one gene to another. For instance, the gene PA4655 (*hemH*) responded relatively slower than PA1249 (*aprA*). Therefore, in order to catch the fast response of PA1249, one needs to measure even more frequently than one needs to perform for PA4655.

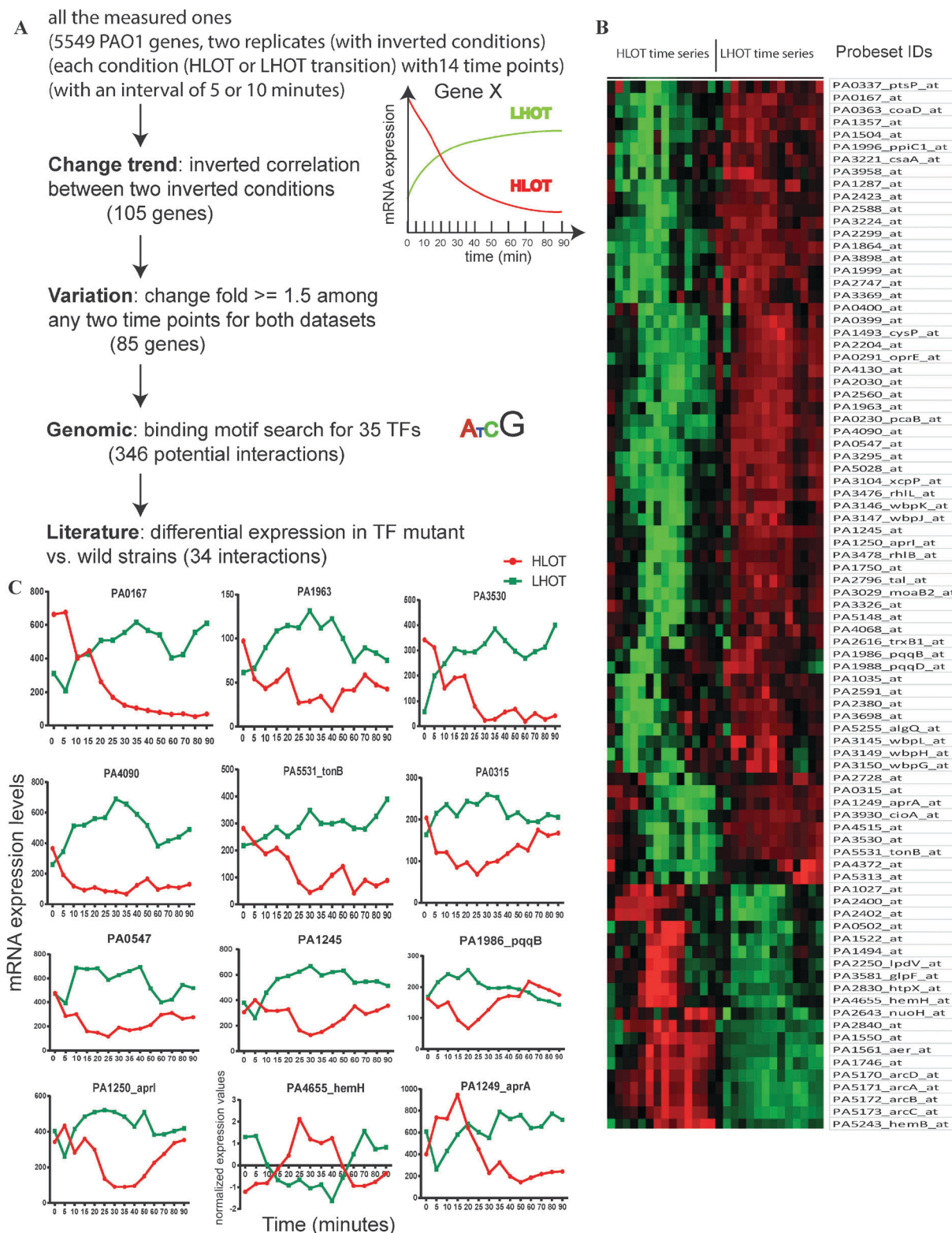


Fig. 1 Strategy for identifying essential responsive genes and constructing a reliable network. (A) An integrative strategy for identifying EORGs from inverted HTR transcriptome data and constructing the transcription regulatory network. (B) The heat map resulting from hierarchical clustering of the identified 85 EORGs. The hierarchical clustering was performed based on \log_2 -transformed expression change ratios (relative to the expression value at time zero of a gene) using average linkage and centered Pearson correlation distance measurements by using the software *cluster* 3.0.⁵⁰ Red indicates positive values (\log_2 transformed); green, negative values; black, zero; lighter and darker red (green) for lower and higher increased (decreased) values, respectively. The original time-series expression values and the negative Pearson correlation *P*-values for each EORG are provided in Table S4 (ESI[†]). (C) Demonstration of various inverted dynamic patterns of selected genes from panel B. Of note, only the gene PA4655 is displayed as the normalized expression values by normalizing the original expression levels from each time course into the data with a mean of zero and a standard deviation of 1.

Among the 85 EORGs, we found some well-known oxygen-availability responders, for instance, the gene cluster (*arcDABC* and *PA5170-3*, Fig. 1B) that encode enzymes for arginine fermentation.²⁹ Although *arcDABC* showed a fast dynamic transcription response during the HLOT transition, their expression peaked three times and still kept much higher (except for that at 90 min) even after contraction than that at time zero during the 90 min sampling period. This might easily explain why the observation of the anaerobic induction of *arc* genes can be shared by others³⁰ as well as by us in this work. The list also includes other interesting genes *e.g.*, *rhIL* (*PA3476*, Fig. 1B), a critical *rhL* quorum sensing component, which is known to be repressed in anaerobic growth.³¹ We also observed a significant reduction of this gene expression during the HLOT transition although the expression levels of *rhIL* were then gradually increased, which were still much lower than that before the oxygen-availability transition. However, the repression of the gene for rhamnosyl transferase B (*rhIB*) (*PA3478*, Fig. 1B), another important quorum sensing gene, was only observed in this work. This is due to the fact that although the expression of *rhIB* was gradually decreased to a quite low level, the expression was then gradually increased starting from 30 min to a similar level as that at time zero. It is not trivial that many people pay attention to the expression dynamics in the first 30 min and consequently easily miss it.

In addition to genes expected, we also identified many other new EORGs. For example, the genes in the operon *wbpLKJHG* (*PA3145-50*, Fig. 1B) showed very fast dynamics and after 90 min returned to levels similar to those before the oxygen-availability transitions. The fast expression dynamics of these new candidates might explain why others cannot notice them mainly due to a relatively low-frequency measurement which has almost no chance to catch fast dynamic responses as discussed above. *WbpL*, a transferase, is necessary for initiating both A- and B-band lipopolysaccharide (LPS) synthesis³² while other genes in this operon were not well characterized yet. Interestingly, we have previously observed the formation alterations of LPS on the surface of PA under oxygen stress conditions although not digging into the individual genes.²⁰ In fact, in previous work we observed an inverted response of the B-band while increasing or decreasing oxygen availability, which exactly fits with our expression data that *wbpL* quickly decreased and then rebounded immediately under the HLOT conditions while quickly increased and then recoiled immediately under the LHOT conditions. Furthermore, since one has almost no chance to randomly obtain the whole operon, which strictly reversely responded to both inverted oxygen-availability transitions, the genes in the *wbpLKJHG* operon represent very promising candidates for oxygen-availability responses. Another couple of genes, which were clustered together due to similar expression patterns in both conditions, worthy to be mentioned, *e.g.*, *qppBD*, (*PA1986* and *PA1988*, pyrroloquinoline quinone biosynthesis protein B and D, Fig. 1B and C) were gradually down-regulated and then rebounded during the HLOT transition while showing an inverted change trend in the LHOT transition. Since pyrroloquinoline quinone in bacteria has been found to play a

critical anti-oxidative role under oxidative stress,³³ these two genes might be another set of interesting candidates playing important roles in response to oxygen availability for PA.

Identification of a highly reliable responsive transcription network

Following the discovery of the EORGs, we seek to identify the transcription regulatory network controlling them and understand the underlying molecular mechanism by which PA responds to oxygen availability. Since transcription factors normally do not change a lot in transcription levels³⁴ and are mainly modified in post-transcription levels, it is not so straightforward to identify a clear correlation between TFs and their target genes even when considering expression time shifts as we and others discovered.¹⁴ When time shifts among a combination of several TFs were considered, more plausible results can be obtained as demonstrated by us and others.³⁵ However, we do not have repeated time-series measurements on any of the two transitions and consequently cannot make a reliable conclusion for a single transition. We therefore utilized binding motifs search approaches to examine the promoter area of all the EORGs from two inverted transitions for 39 TFs with experimentally-verified binding motifs (Table S3, ESI†). Four out of the 39 TFs were considered to be apparently absent and were consequently excluded due to extremely low expression levels (see Methods). The pattern matching tool *matrix scan*³⁶ was used for computational prediction of binding motifs located on the regulatory sequences 1000 bps upstream to the coding sequence of all the EORGs considered in this study.³⁶ The tool inferred 346 potential regulatory interactions (Table S1, ESI†). We then further narrowed down the list of potential regulatory interactions to a more realistic list of interactions by only extracting those potential interactions, in which literature has already shown that the mutant or overexpression of the TF has significant effects on the transcription expression of the target gene as measured by transcriptomic and/or chromatin immunoprecipitation (ChIP)-chip approaches. Eventually, we identified 34 transcription regulatory interactions (Fig. 1A). Surprisingly, we found that only the regulatory subnetworks controlled by the well-known oxygen-responsive TFs showed a very high consistence between the inferred potential regulatory network and literature knowledge. Especially, we found that 7 out of the 8 transcription regulatory interactions (87.5%, $P\text{-value} = 2.7 \times 10^{-12}$, cumulative binomial distribution, in total, 92 target genes are reported as summarized in Table S1, ESI†) in the inferred subnetwork controlled by ANR were consistent with the literature (Fig. 2). Five out of the total 6 inferred target genes (83.3%, $P\text{-value} = 6.1 \times 10^{-6}$, Fig. 2, 355 target genes are reported) regulated by a quorum sensing regulator *RhlR* are known to be regulated by *RhlR* or affected by *RhlR* mutants. In fact, another quorum sensing regulator *LasR* also showed a quite high consistency; 8 out of the 17 potential regulatory interactions ($P\text{-value} = 6.1 \times 10^{-6}$, 375 target genes reported) controlled by *LasR* were overlapped between literature knowledge and the list of the 34 interactions (Fig. 2). Furthermore, we observed that 4 out of 10 potential regulatory interactions ($P\text{-value} = 5.0 \times 10^{-7}$, only 39 target genes reported)

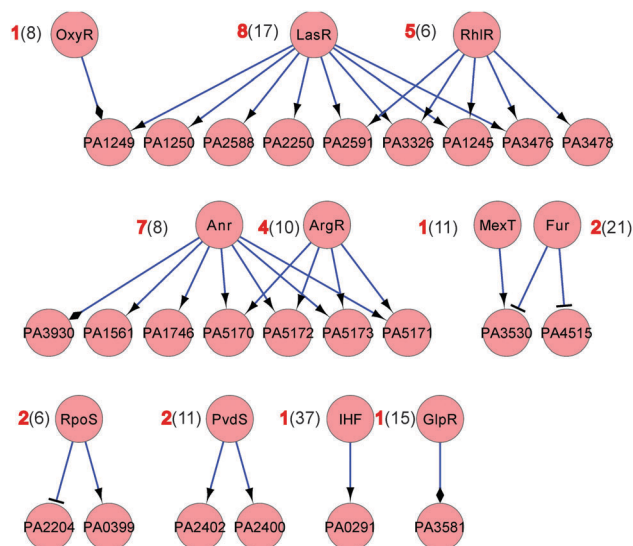


Fig. 2 A reliable transcription regulatory network of PA in response to oxygen-availability changes. The red and black numbers in the bracket correspond to the number of interactions controlled by a given TF in the current literature-confirmed regulatory network and in the predicted regulatory network (Table S1, ESI[†]), respectively. The arrow represents a positive regulation; the diamond arrow indicates a regulation but with unknown effects; another type represents an inhibitory regulation.

regulated by ArgR belonged to the final 34 interactions. Actually, anaerobic expression of *arcDABC* (*PA5170-3*) has been shown to be ANR-dependent and is stimulated further by the arginine-responsive regulator ArgR (*PA0893*).³⁷ Notably, our network showed exactly a combinatory transcription regulation between ArgR and Anr on *arcDABC* (Fig. 2). Furthermore, the relevance of the identified 34 interactions was supported by the similarity in the expression patterns between the co-regulated genes as they were closely clustered (Fig. 1B). The evidence independently increases the confidence level since we did not use coexpression information when predicting the network as discussed above. For instance, the genes *PA1561*, *PA1746* and *arcDABC*, which were all predicted to be regulated by ANR, were tightly clustered together. The two genes *PA4515* and *PA3530* co-regulated by fur (the ferric uptake regulator, *PA4764*) (Fig. 2) were next to each other (Fig. 1B). The target genes of PvdS (the sigma factor required for pyoverdine synthesis,³⁸ *PA2426*) from our predicted network, *PA2400* and *PA2402*, also remained in the vicinity of the cluster tree. So did *PA0399* and *PA2204*, the target genes of RpoS (the alternative sigma factor,³⁹ *PA3622*).

In order to check whether these high percentages were biased by the high number of known target genes for these TFs aforementioned, we also evaluated whether a high number of target genes were also known to be affected by other TFs, which are, however, not reported to be directly involved in oxygen-availability regulatory responses. For example, FleQ, a transcriptional activator belonging to the NtrC subfamily of response regulators, involved in the regulation of mucin adhesion and flagellar expression⁴⁰ and PsrA, a positive transcriptional regulator of the type III secretion system⁴¹ affect 146 and 204 target genes, respectively, according to our knowledge

(Table S2, ESI[†]). Both FleQ and PsrA are not directly linked to oxygen-availability responses. We inferred 6 and 8 potential regulatory interactions for FleQ and PsrA, respectively. As indicated above, the number of their known target genes is even higher than that of many well-known oxygen-responsive TFs. However, we hardly identified any overlap between genes potentially regulated by them and those reported in literature. These data showed that a high percentage overlap was not biased due to a high number of known target genes for the given TFs.

To find more evidence supporting the reliability of the inferred regulatory network, we also checked the minority of the regulatory network predicted to be regulated by potential oxygen-responsive TFs. The ferric uptake regulator (*fur*) apparently affects the aerobic growth but not the microaerobic growth of PA.⁴² This phenotype indicates that *fur* plays a role in asymmetric regulation under the two opposite conditions, further consolidated by the discovery that its mutants affect the expression of some genes in distinct ways between the aerobic and anaerobic environments.⁴³ We would like to examine whether the number of inferred regulatory interactions controlled by *fur* matching with literature knowledge could be obtained by chance. Interestingly, 2 out of the 21 inferred regulatory interactions matched with literature information (P -value = 0.01, Tables S1 and S2, ESI[†]) but the matched percentage is far from those for Anr and RhlR. These results demonstrate that the predicted regulatory network is still quite accurate for the potentially responsive TFs although the observed accuracy might not be as high as that for apparently affected TFs, e.g., ANR and RhlR. The two predicted target genes (*PA3530*, encoding ferredoxin, and *PA4515*) were reported to be strongly upregulated upon iron starvation,⁴⁴ indicating a *fur* regulation on them since *FUR* repression is relieved under iron starvation. Moreover, the two genes clustered gapless (Fig. 1B), supporting a coregulation. As discussed above (Fig. 1C), the expression levels of *PA3530* and *PA4515* gradually decreased in the HLOT transition but increased in another transition, indicating an essential role in aerobic but not in anaerobic conditions for the two genes, which fits well with the observation that their expression regulator (*fur*) plays an important role in aerobic but not in anaerobic environments.⁴² We also checked the other predicted *fur* targets, which were not yet reported to be affected by *fur* (Table S1, ESI[†]). Interestingly, the genes *PA5170-3* (*arcDABC*) were also predicted to be controlled by *fur*. Although none of them have been found to be regulated by *fur* compared with some related reports,⁴⁴⁻⁴⁶ they were clustered tightly due to their similar expression patterns (Fig. 1B). In addition, the binding motifs of *fur* were found in the promoter area of these genes and these genes showed a significantly inverted expression pattern between the two opposite conditions, which collectively suggests that the *arcDABC* genes were very likely to be co-regulated by *fur* in response to oxygen availability. Except for those listed in Table S4 (ESI[†]), most of the reported *fur*-regulated genes did not show a significantly inverted correlation between the two opposite transitions and therefore were not included as EORGs. This is understandable in that *fur* plays an asymmetric role between the two opposite conditions and

therefore many of the fur-regulated genes did not respond inversely. Another tiny fraction of the inferred interactions was predicted to be controlled by OxyR, the oxidative stress regulator, which plays a crucial role in oxidative stress defense.^{47,48} But only AprA (the alkaline metalloproteinase, a virulent factor, PA1249) out of the 8 predicted target genes has been observed to be regulated by OxyR as compared to the results detected by the ChIP–chip approach⁴⁹ or by other traditional methods⁴⁷ (not significant, Tables S1 and S2, ESI†). This is not surprising since the authors used H₂O₂ to stress PA, which obviously generated distinct regulatory responses as we challenged PA under oxygen-availability transitions. Cumulatively, all the evidence aforementioned support that the list of the 346 predicted regulatory interactions (Table S1, ESI†) represent a highly reliable regulatory network, especially those subnetworks regulated by apparently affected TFs under the studied conditions although many of them were not yet experimentally reported.

Conclusions

Our work has demonstrated the power of using replicate time-series data generated under inverted conditions to construct a highly accurate oxygen availability responsive network of PA. We have also identified the EORGs by utilizing the HTR data from the two inverted conditions, which are exclusively available in our work. As shown in this work, the fast dynamic responsive expression pattern of many new EORGs cannot be discovered unless with such a high frequent measurement as performed here. Last but not least, we have found that it might be only feasible to identify an accurate network for TFs which are apparently affected (activated or inhibited) under the given conditions but hardly plausible for many other expressed TFs on a genome scale. Therefore, the efforts focusing on certain TFs apparently affected under the given conditions might be more productive. We believe that this discovery might be generally applicable for network construction of various cell types under various physiological or pathological conditions.

Methods

Cultivation conditions and time-series dynamic experiments

P. aeruginosa PAO1 from glycerol stock (−80 °C) was activated in a shaking flask at 37 °C for 14 hours with medium B, which contains per liter 20 g of glucose, 6 g of yeast extract, 0.6 g of (NH₄)₂SO₄, 2 g of Na₂HPO₄, 0.3 g of MgSO₄·7H₂O, and pH adjusted to 7.0 with 1 M NaOH (Mian *et al.*, 1978).⁵¹ The pre-culture was then transferred into a shaking flask with medium A containing per liter 20 g of sodium gluconate, 20 g of sodium glutamate, 3 g of Na₂HPO₄, 0.3 g of MgSO₄·7H₂O, and pH adjusted to 7.0 with 1 M NaOH⁵¹ at an inoculation ratio of 10% and cultivated under the same conditions for another 13 hours. The final concentration of nitrate (in the order of μM) due to the presence of yeast extract⁵² was almost negligible.

A 2.5 L stirred tank bioreactor (Applikon Biotechnology, Netherlands) containing 1.8 L of glucose minimal medium with low iron concentration described elsewhere,¹⁸ except an

initial concentration of 5 g L^{−1} glucose, was prepared. The dissolved oxygen concentration (pO₂) measured using a Clark pO₂ electrode was calibrated as 100% with press air after autoclaving the medium under the experimental conditions. The second seed culture was inoculated into the bioreactor to an initial OD of 0.05 at 600 nm wavelength. The stirrer speed, pH and temperature were controlled at 300 rpm, pH 7.0 (by adding 2 M NaOH) and 37 °C, respectively, throughout the batch phase and the chemostat cultivation by a real-time computer control system UBICON (Universal Bioprocess Control System, ESD, Hanover, Germany). The pO₂ was controlled at 100% air saturation in the batch phase and varied during chemostat cultivation by dynamically adjusting the ratio of pure nitrogen and pure oxygen *via* two mass flow controllers and controlled by the UBICON system. The total aeration rate was kept at a constant value of 1 VVM by the control system UBICON. After 5.5 hours of batch cultivation, the cultivation was shifted to the continuous mode by continuously feeding medium C, which was similar to the glucose minimal medium mentioned above but containing 1.5 g L^{−1} glucose, at a fixed rate to ensure a dilution rate of 0.2 h^{−1}. The culture volume in the bioreactor was controlled at exactly 1.5 L using an effluent pump controlled by a balance for the whole bioreactor system. After medium exchange of at least four bioreactor volumes while keeping the pO₂ constant at 100% air saturation, the system reached its first steady state, as indicated by constant CO₂ release. After first sampling, the controlled pO₂ value was set to 0.5% and regulated by a proportional-integral-derivative (PID) controller of the UBICON system. The pO₂ value rapidly dropped to about 1.0% in less than 5 minutes (Fig. S1, ESI†) and controlled in the range of 0.5–1.0% air saturation afterwards. Sampling for transcriptome analysis was started before the switching of the pO₂ value (defined as time point zero). In total, 14 samples were harvested at time points 0, 5, 10, 15, 20, 25, 30, 35, 40, 50, 60, 70, 80 and 90 min after switching from aerobic to microaerobic conditions. After reaching a steady state (after about another four bioreactor volume exchange) under these conditions, the culture was shifted from microaerobic back to fully aerobic conditions (pO₂ set point value from 0.5% to 100%). A similar set of samples were taken during the reversed transition with the same time intervals.

RNA isolation, microarray analysis of gene expression and data preprocessing

In order to stabilize RNA immediately, the samples from the chemostat culture of PA were directly flushed into a pre-cooled RNAProtect Bacteria Reagent (Qiagen) and treated instantly as suggested by the supplier before storing at −80 °C for later RNA isolation. The total RNA was extracted by using the RNeasy mini kit including an on-column DNase treatment according to the manufacturer's instructions (Qiagen). The RNA concentration and purity were determined using the 2100 Bioanalyser (Agilent). A total of 10 μg of each experimental RNA sample was used for cDNA synthesis with Superscript II reverse transcriptase (Invitrogen, Carlsbad, CA). DNaseI (Pierce) and 10-fold One-Phor-All Buffer (GE healthcare) were used for cDNA fragmentation. The Enzo BioArray terminal labeling kit (Affymetrix) was used for labeling

the fragmented cDNA with a size range from 50–200 bp. The fragmentation and labeling effects were checked by gel electrophoresis. The cDNA was loaded onto Affymetrix PA GeneChip. Target hybridization was performed at 37 °C for 16 hours by using a GeneChip Hybridization Oven 640. Chip washing and staining were performed using an Affymetrix GeneChip Fluidics Station 400 and chips were scanned using an Agilent Genearray Scanner. The scanned images were analyzed using the Affymetrix GCOS program. The data were analyzed using Microarray Suite version 5.0 (MAS 5.0) using Affymetrix default analysis settings and global scaling as a normalization method. The trimmed mean target intensity of each array was set to 150. Probe sets that were absent in all the time-series samples according to Affymetrix flags were removed. Probes with intensities lower than 50 at each time point were excluded.^{53,54} In addition to the rules described above, the regulators were defined as absence if the average expression values were less than 50 at any of the two inverted transitions. *Via* these rules, we excluded Dnr, PchR, PhhR and TrpI from the list of 39 TFs. The standard centered Pearson correlation coefficient was used to evaluate whether the expression patterns are inverted or not between the two opposite transitions. Before the Pearson correlation coefficient was calculated, each gene was normalized separately (mean of 0 and standard deviation of 1) for each individual time series data. The *P*-value was determined based on the correlation coefficient distribution curve (Table S4, ESI†) resulting from randomly shuffled data of the original data sets.

Searching of transcription binding motifs

Experimentally verified binding motifs for 39 different PA TFs and operon information were retrieved from databases such as RegTransBase (<http://regtransbase.lbl.gov/cgi-bin/regtransbase?page=main>) and Prodoric (www.prodoric.de) and also from literature sources and publications (Table S3, ESI†). They were used to construct the corresponding Position Specific Scoring Matrices (PSSMs) using the tool *consensus* (<http://rsat.ulb.ac.be/rsat/>). The online pattern matching tool *matrix scan*³⁶ was used for computational prediction of binding motifs located on the regulatory sequences 1000 bps upstream to the coding sequence of potential target genes or their corresponding operons considered in this study.³⁶ A pseudo-count value of 1 was employed to overcome any bias in cases where a small number of validated binding sites (less than 3) were used to construct a PSSM. A background model (consisting of a whole genome subset of upstream regulatory regions with no overlap with open reading frames) was used to estimate the probability for each site to occur by chance rather than as an instance of the motif itself. The tool *matrix scan* supports background models with arbitrary Markov order *m* (we here used 4, which explains the dependence of one residue on the 4 preceding residues). All potential sites which have *P*-values smaller than 0.0001 were considered as predicted motifs.

Data availability

The complete time-series microarray data set (28 arrays) is available in the Gene Expression Omnibus (GSE52445).

Authors' contributions

FH designed and performed high-time-resolution expression analysis, network construction and interpretation. WW analyzed the biological significance. PZ, WW and JS performed the fermentation and microarray experiments. PS performed binding motif analysis. FH and WW drafted the manuscript. AZ supervised the study and revised the manuscript.

Acknowledgements

This work was supported partially by a DFG project granted to AZ within the Key Research Area 1316. FH was supported by German Helmholtz Association and partially by Luxembourg Centre for Systems Biomedicine. We acknowledge Robert Geffers for microarray measurements.

References

- 1 D. Worlitzsch, R. Tarran, M. Ulrich, U. Schwab, A. Cekici, K. C. Meyer, P. Birrer, G. Bellon, J. Berger, T. Weiss, K. Botzenhart, J. R. Yankaskas, S. Randell, R. C. Boucher and G. Doring, Effects of reduced mucus oxygen concentration in airway *Pseudomonas* infections of cystic fibrosis patients, *J. Clin. Invest.*, 2002, **109**, 317–325.
- 2 S. S. Yoon, R. F. Hennigan, G. M. Hilliard, U. A. Ochsner, K. Parvatiyar, M. C. Kamani, H. L. Allen, T. R. DeKievit, P. R. Gardner, U. Schwab, J. J. Rowe, B. H. Iglewski, T. R. McDermott, R. P. Mason, D. J. Wozniak, R. E. Hancock, M. R. Parsek, T. L. Noah, R. C. Boucher and D. J. Hassett, *Pseudomonas aeruginosa* anaerobic respiration in biofilms: relationships to cystic fibrosis pathogenesis, *Dev. Cell*, 2002, **3**, 593–603.
- 3 J. O'Callaghan, F. J. Reen, C. Adams and F. O'Gara, Low oxygen induces the type III secretion system in *Pseudomonas aeruginosa* via modulation of the small RNAs rsmZ and rsmY, *Microbiology*, 2011, **157**, 3417–3428.
- 4 C. Alvarez-Ortega and C. S. Harwood, Responses of *Pseudomonas aeruginosa* to low oxygen indicate that growth in the cystic fibrosis lung is by aerobic respiration, *Mol. Microbiol.*, 2007, **65**, 153–165.
- 5 V. E. Wagner, D. Bushnell, L. Passador, A. I. Brooks and B. H. Iglewski, Microarray analysis of *Pseudomonas aeruginosa* quorum-sensing regulons: effects of growth phase and environment, *J. Bacteriol.*, 2003, **185**, 2080–2095.
- 6 R. W. Ye, D. Haas, J. O. Ka, V. Krishnapillai, A. Zimmermann, C. Baird and J. M. Tiedje, Anaerobic activation of the entire denitrification pathway in *Pseudomonas aeruginosa* requires Anr, an analog of Fnr, *J. Bacteriol.*, 1995, **177**, 3606–3609.
- 7 A. Zimmermann, C. Reimann, M. Galimand and D. Haas, Anaerobic growth and cyanide synthesis of *Pseudomonas aeruginosa* depend on anr, a regulatory gene homologous with fnr of *Escherichia coli*, *Mol. Microbiol.*, 1991, **5**, 1483–1490.
- 8 D. Balasubramanian and K. Mathee, Comparative transcriptome analyses of *Pseudomonas aeruginosa*, *Hum. Genomics*, 2009, **3**, 349–361.

- 9 K. Trunk, B. Benkert, N. Quack, R. Munch, M. Scheer, J. Garbe, L. Jansch, M. Trost, J. Wehland, J. Buer, M. Jahn, M. Schobert and D. Jahn, Anaerobic adaptation in *Pseudomonas aeruginosa*: definition of the Anr and Dnr regulons, *Environ. Microbiol.*, 2010, **12**, 1719–1733.
- 10 M. D. Platt, M. J. Schurr, K. Sauer, G. Vazquez, I. Kukavica-Ibrulj, E. Potvin, R. C. Levesque, A. Fedynak, F. S. Brinkman, J. Schurr, S. H. Hwang, G. W. Lau, P. A. Limbach, J. J. Rowe, M. A. Lieberman, N. Barraud, J. Webb, S. Kjelleberg, D. F. Hunt and D. J. Hassett, Proteomic, microarray, and signature-tagged mutagenesis analyses of anaerobic *Pseudomonas aeruginosa* at pH 6.5, likely representing chronic, late-stage cystic fibrosis airway conditions, *J. Bacteriol.*, 2008, **190**, 2739–2758.
- 11 M. Wu, T. Guina, M. Brittnacher, H. Nguyen, J. Eng and S. I. Miller, The *Pseudomonas aeruginosa* proteome during anaerobic growth, *J. Bacteriol.*, 2005, **187**, 8185–8190.
- 12 K. S. Williamson, L. A. Richards, A. C. Perez-Osorio, B. Pitts, K. McInnerney, P. S. Stewart and M. J. Franklin, Heterogeneity in *Pseudomonas aeruginosa* biofilms includes expression of ribosome hibernation factors in the antibiotic-tolerant subpopulation and hypoxia-induced stress response in the metabolically active population, *J. Bacteriol.*, 2012, **194**, 2062–2073.
- 13 E. Sonnleitner, N. Gonzalez, T. Sorger-Domenigg, S. Heeb, A. S. Richter, R. Backofen, P. Williams, A. Huttenhofer, D. Haas and U. Blasi, The small RNA PhrS stimulates synthesis of the *Pseudomonas aeruginosa* quinolone signal, *Mol. Microbiol.*, 2011, **80**, 868–885.
- 14 F. He, R. Balling and A. P. Zeng, Reverse engineering and verification of gene networks: principles, assumptions, and limitations of present methods and future perspectives, *J. Biotechnol.*, 2009, **144**, 190–203.
- 15 F. He, H. Chen, M. Probst-Kepper, R. Geffers, S. Eifes, A. Del Sol, K. Schughart, A. P. Zeng and R. Balling, PLAU inferred from a correlation network is critical for suppressor function of regulatory T cells, *Mol. Syst. Biol.*, 2012, **8**, 624.
- 16 E. J. Kim, W. Wang, W. D. Deckwer and A. P. Zeng, Expression of the quorum-sensing regulatory protein LasR is strongly affected by iron and oxygen concentrations in cultures of *Pseudomonas aeruginosa* irrespective of cell density, *Microbiology*, 2005, **151**, 1127–1138.
- 17 P. Zheng, J. Sun, R. Geffers and A. P. Zeng, Functional characterization of the gene PA2384 in large-scale gene regulation in response to iron starvation in *Pseudomonas aeruginosa*, *J. Biotechnol.*, 2007, **132**, 342–352.
- 18 W. Sabra, E. J. Kim and A. P. Zeng, Physiological responses of *Pseudomonas aeruginosa* PAO1 to oxidative stress in controlled microaerobic and aerobic cultures, *Microbiology*, 2002, **148**, 3195–3202.
- 19 E. J. Kim, W. Sabra and A. P. Zeng, Iron deficiency leads to inhibition of oxygen transfer and enhanced formation of virulence factors in cultures of *Pseudomonas aeruginosa* PAO1, *Microbiology*, 2003, **149**, 2627–2634.
- 20 W. Sabra, H. Lunsdorf and A. P. Zeng, Alterations in the formation of lipopolysaccharide and membrane vesicles on the surface of *Pseudomonas aeruginosa* PAO1 under oxygen stress conditions, *Microbiology*, 2003, **149**, 2789–2795.
- 21 C. F. Quo, C. Kaddi, J. H. Phan, A. Zollanvari, M. Xu, M. D. Wang and G. Alterovitz, Reverse engineering biomolecular systems using -omic data: challenges, progress and opportunities, *Briefings Bioinf.*, 2012, **13**, 430–445.
- 22 K. Y. Yeung, K. M. Dombek, K. Lo, J. E. Mittler, J. Zhu, E. E. Schadt, R. E. Bumgarner and A. E. Raftery, Construction of regulatory networks using expression time-series data of a genotyped population, *Proc. Natl. Acad. Sci. U. S. A.*, 2011, **108**, 19436–19441.
- 23 D. Marbach, J. C. Costello, R. Kuffner, N. M. Vega, R. J. Prill, D. M. Camacho, K. R. Allison, M. Kellis, J. J. Collins and G. Stolovitzky, Wisdom of crowds for robust gene network inference, *Nat. Methods*, 2012, **9**, 796–804.
- 24 A. Crombach, K. R. Wotton, D. Cicin-Sain, M. Ashyraliyev and J. Jaeger, Efficient reverse-engineering of a developmental gene regulatory network, *PLoS Comput. Biol.*, 2012, **8**, e1002589.
- 25 R. Bonneau, M. T. Facciotti, D. J. Reiss, A. K. Schmid, M. Pan, A. Kaur, V. Thorsson, P. Shannon, M. H. Johnson, J. C. Bare, W. Longabaugh, M. Vuthoori, K. Whitehead, A. Madar, L. Suzuki, T. Mori, D. E. Chang, J. Diruggiero, C. H. Johnson, L. Hood and N. S. Baliga, A predictive model for transcriptional control of physiology in a free living cell, *Cell*, 2007, **131**, 1354–1365.
- 26 A. Tjarnberg, T. E. Nordling, M. Studham and E. L. Sonnhammer, Optimal sparsity criteria for network inference, *J. Comput. Biol.*, 2013, **20**, 398–408.
- 27 A. J. Walhout, What does biologically meaningful mean? A perspective on gene regulatory network validation, *Genome Biol.*, 2011, **12**, 109.
- 28 S. R. Maetschke, P. B. Madhamshettiwar, M. J. Davis and M. A. Ragan, Supervised, semi-supervised and unsupervised inference of gene regulatory networks, *Briefings Bioinf.*, 2013, DOI: 10.1093/bib/bbt034.
- 29 C. Vander Wauven, A. Pierard, M. Kley-Raymann and D. Haas, *Pseudomonas aeruginosa* mutants affected in anaerobic growth on arginine: evidence for a four-gene cluster encoding the arginine deiminase pathway, *J. Bacteriol.*, 1984, **160**, 928–934.
- 30 H. V. Winteler, B. Schneidinger, K. E. Jaeger and D. Haas, Anaerobically controlled expression system derived from the arcDABC operon of *Pseudomonas aeruginosa*: application to lipase production, *Appl. Environ. Microbiol.*, 1996, **62**, 3391–3398.
- 31 M. J. Filiatrault, V. E. Wagner, D. Bushnell, C. G. Haidaris, B. H. Iglewski and L. Passador, Effect of anaerobiosis and nitrate on gene expression in *Pseudomonas aeruginosa*, *Infect. Immun.*, 2005, **73**, 3764–3772.
- 32 H. L. Rocchetta, L. L. Burrows, J. C. Pacan and J. S. Lam, Three rhamnosyltransferases responsible for assembly of the A-band D-rhamnan polysaccharide in *Pseudomonas aeruginosa*: a fourth transferase, WbpL, is required for the initiation of both A-band and B-band lipopolysaccharide synthesis, *Mol. Microbiol.*, 1998, **28**, 1103–1119.

- 33 H. S. Misra, N. P. Khairnar, A. Barik, K. Indira Priyadarsini, H. Mohan and S. K. Apte, Pyrroloquinoline-quinone: a reactive oxygen species scavenger in bacteria, *FEBS Lett.*, 2004, **578**, 26–30.
- 34 Z. Bar-Joseph, A. Gitter and I. Simon, Studying and modeling dynamic biological processes using time-series gene expression data, *Nat. Rev. Genet.*, 2012, **13**, 552–564.
- 35 M. E. Manioudaki and P. Poirazi, Modeling regulatory cascades using Artificial Neural Networks: the case of transcriptional regulatory networks shaped during the yeast stress response, *Front. Genet.*, 2013, **4**, 110.
- 36 J. V. Turatsinze, M. Thomas-Chollier, M. Defrance and J. van Helden, Using RSAT to scan genome sequences for transcription factor binding sites and cis-regulatory modules, *Nat. Protoc.*, 2008, **3**, 1578–1588.
- 37 C. D. Lu, H. Winteler, A. Abdelal and D. Haas, The ArgR regulatory protein, a helper to the anaerobic regulator ANR during transcriptional activation of the arcD promoter in *Pseudomonas aeruginosa*, *J. Bacteriol.*, 1999, **181**, 2459–2464.
- 38 M. J. Wilson, B. J. McMorran and I. L. Lamont, Analysis of promoters recognized by PvdS, an extracytoplasmic-function sigma factor protein from *Pseudomonas aeruginosa*, *J. Bacteriol.*, 2001, **183**, 2151–2155.
- 39 K. Barkovits, A. Harms, C. Benkartek, J. L. Smart and N. Frankenberg-Dinkel, Expression of the phytochrome operon in *Pseudomonas aeruginosa* is dependent on the alternative sigma factor RpoS, *FEMS Microbiol. Lett.*, 2008, **280**, 160–168.
- 40 S. K. Arora, B. W. Ritchings, E. C. Almira, S. Lory and R. Ramphal, A transcriptional activator, FleQ, regulates mucin adhesion and flagellar gene expression in *Pseudomonas aeruginosa* in a cascade manner, *J. Bacteriol.*, 1997, **179**, 5574–5581.
- 41 D. K. Shen, D. Filopon, L. Kuhn, B. Polack and B. Toussaint, PsrA is a positive transcriptional regulator of the type III secretion system in *Pseudomonas aeruginosa*, *Infect. Immun.*, 2006, **74**, 1121–1129.
- 42 D. J. Hassett, P. A. Sokol, M. L. Howell, J. F. Ma, H. T. Schweizer, U. Ochsner and M. L. Vasil, Ferric uptake regulator (Fur) mutants of *Pseudomonas aeruginosa* demonstrate defective siderophore-mediated iron uptake, altered aerobic growth, and decreased superoxide dismutase and catalase activities, *J. Bacteriol.*, 1996, **178**, 3996–4003.
- 43 H. A. Barton, Z. Johnson, C. D. Cox, A. I. Vasil and M. L. Vasil, Ferric uptake regulator mutants of *Pseudomonas aeruginosa* with distinct alterations in the iron-dependent repression of exotoxin A and siderophores in aerobic and microaerobic environments, *Mol. Microbiol.*, 1996, **21**, 1001–1017.
- 44 U. A. Ochsner, P. J. Wilderman, A. I. Vasil and M. L. Vasil, GeneChip expression analysis of the iron starvation response in *Pseudomonas aeruginosa*: identification of novel pyoverdine biosynthesis genes, *Mol. Microbiol.*, 2002, **45**, 1277–1287.
- 45 U. A. Ochsner and M. L. Vasil, Gene repression by the ferric uptake regulator in *Pseudomonas aeruginosa*: cycle selection of iron-regulated genes, *Proc. Natl. Acad. Sci. U. S. A.*, 1996, **93**, 4409–4414.
- 46 U. A. Ochsner, Z. Johnson and M. L. Vasil, Genetics and regulation of two distinct haem-uptake systems, phu and has, in *Pseudomonas aeruginosa*, *Microbiology*, 2000, **146**(Pt 1), 185–198.
- 47 U. A. Ochsner, M. L. Vasil, E. Alsabbagh, K. Parvatiyar and D. J. Hassett, Role of the *Pseudomonas aeruginosa* oxyR-recG operon in oxidative stress defense and DNA repair: OxyR-dependent regulation of katB-ankB, ahpB, and ahpC-ahpF, *J. Bacteriol.*, 2000, **182**, 4533–4544.
- 48 T. Vinckx, S. Matthijs and P. Cornelis, Loss of the oxidative stress regulator OxyR in *Pseudomonas aeruginosa* PAO1 impairs growth under iron-limited conditions, *FEMS Microbiol. Lett.*, 2008, **288**, 258–265.
- 49 Q. Wei, P. N. Minh, A. Dotsch, F. Hildebrand, W. Panmanee, A. Elfarash, S. Schulz, S. Plaisance, D. Charlier, D. Hassett, S. Haussler and P. Cornelis, Global regulation of gene expression by OxyR in an important human opportunistic pathogen, *Nucleic Acids Res.*, 2012, **40**, 4320–4333.
- 50 M. J. de Hoon, S. Imoto, J. Nolan and S. Miyano, Open source clustering software, *Bioinformatics*, 2004, **20**, 1453–1454.
- 51 F. A. Mian, T. R. Jarman and R. C. Righelato, Biosynthesis of exopolysaccharide by *Pseudomonas aeruginosa*, *J. Bacteriol.*, 1978, **134**, 418–422.
- 52 J. Xu, X. Xu and W. Verstraete, Adaptation of *E. coli* cell method for micro-scale nitrate measurement with the Griess reaction in culture media, *J. Microbiol. Methods*, 2000, **41**, 23–33.
- 53 J. Ambroise, B. Bearzatto, A. Robert, B. Govaerts, B. Macq and J. L. Gala, Impact of the spotted microarray preprocessing method on fold-change compression and variance stability, *BMC Bioinf.*, 2011, **12**, 413.
- 54 I. Amit, A. Citri, T. Shay, Y. Lu, M. Katz, F. Zhang, G. Tarcic, D. Siwak, J. Lahad, J. Jacob-Hirsch, N. Amariglio, N. Vaisman, E. Segal, G. Rechavi, U. Alon, G. Mills, E. Domany and Y. Yarden, A module of negative feedback regulators defines growth factor signaling, *Nat. Genet.*, 2007, **39**, 503–515.